SLAC–PUB–7825
June 1998

A Preliminary Direct Measurement of the Parity Violating Coupling of the Z^0 to Strange Quarks, A_s*

The SLD Collaboration**

Stanford Linear Accelerator Center

Stanford University, Stanford, CA 94309

ABSTRACT

We present a preliminary direct measurement of the parity violating coupling of the Z^0 to strange quarks, A_s, derived from a sample of approximately 300,000 hadronic decays of Z^0 bosons produced with a polarized electron beam and recorded by the SLD experiment at SLAC between 1993 and 1997. $Z^0 \to s\bar{s}$ events are tagged by the presence in each event hemisphere of a high-momentum $K^{\pm}$, K^0_s or $\Lambda^0/\bar{\Lambda}^0$ identified using the Cherenkov Ring Imaging Detector and/or a mass tag. The CCD vertex detector is used to suppress the background from heavy flavor events. The strangeness of the tagged particle is used to sign the event thrust axis in the direction of the initial s quark. The coupling A_s is obtained directly from a measurement of the left-right-forward-backward production asymmetry in polar angle of the tagged s quark. To reduce the model dependence of the measurement, the background from $u\bar{u}$ and $d\bar{d}$ events is measured from the data, as is the analyzing power of the method for $s\bar{s}$ events. We measure $A_s = 0.82 \pm 0.10(stat.) \pm 0.07(syst.)(preliminary)$.

Contributed to the XXIX International Conference on High Energy Physics, Vancouver, B.C. Canada, July 23-29 1998: parallel session 1: 'Electroweak interactions'; plenary session 1: 'Experimental Status of the Standard Model'.

*Work supported by Department of Energy contract DE-AC03-76SF00515 (SLAC).

1. Introduction

Measurements of the fermion production asymmetries in the process $e^+e^- \to Z^0 \to f\bar{f}$ provide information on the extent of parity violation in the coupling of the Z^0 boson to fermions of type f. At Born level, the differential production cross section can be expressed in terms of $x = \cos\theta$, where θ is the polar angle of the final state fermion f with respect to the electron beam direction:

$$\sigma^f(x) = \frac{d\sigma}{dx} \propto (1 - A_e P_e)(1 + x^2) + 2A_f(A_e - P_e)x, \tag{1}$$

where P_e is the longitudinal polarization of the electron beam, the positron beam is assumed unpolarized, and the asymmetry parameters $A_f = 2v_f a_f/(v_f^2 + a_f^2)$ are defined in terms of the vector (v_f) and axial-vector (a_f) couplings of the Z^0 to fermion f. The Standard Model (SM) predictions for the values of the asymmetry parameters, assuming $\sin^2\theta_w = 0.23$, are $A_e = A_\mu = A_\tau = 0.16$, $A_u = A_c = A_t = 0.67$ and $A_d = A_s = A_b = 0.94$.

If one measures the polar angle distribution for a given final state $f\bar{f}$, one can derive the forward-backward production asymmetry:

$$A_{FB}^f = \frac{3}{4}\frac{A_e - P_e}{1 - A_e P_e} A_f \tag{2}$$

which depends on both the initial and final state asymmetry parameters as well as on the beam polarization. For zero polarization, one measures the product of couplings $A_e A_f$, which has a rather small value since $A_e = 0.16$. If one measures the distributions in equal luminosity samples taken with negative and positive beam polarization of magnitude P_e, then one can derive the left-right-forward-backward asymmetry:

$$\tilde{A}_{FB}^f = \frac{3}{4}|P_e| A_f \tag{3}$$

which is insensitive to the initial state coupling.

It is important to measure as many of these asymmetry parameters as possible, in order to test the SM predictions of lepton, up-quark and down-quark universality. A

number of previous measurements have been made by experiments at LEP and SLC of A_e, A_μ, A_τ, A_c and A_b [1]. The leptonic final states are identified easily by their low track multiplicities and identification of the stable leptons. The $c\bar{c}$ final state can be identified by exclusive or partial reconstruction of the leading charmed hadron in a hadronic jet. The $b\bar{b}$ final state can be tagged by the presence of a lepton with high momentum transverse to the jet axis or of a decay vertex displaced from the primary interaction point, indicating the presence of a leading B hadron in the jet. In contrast, very few measurements exist for the light flavor quarks, due to the difficulty of tagging specific light flavors. It has recently been demonstrated experimentally [2] that light flavored jets can be tagged by the presence of a high-momentum 'leading' identified particle that has a valence quark of the desired flavor, for example a K^- (K^+) meson could tag an s ($\bar{s}$) jet. However the background from other light flavors (a $\bar{u}$ jet can also produce a leading K^-), decays of B and D hadrons, and nonleading kaons in events of all flavors is large, and neither the signal nor the background has been well measured experimentally.

The DELPHI collaboration has measured [3] the polar angle production asymmetries of $K^\pm$ mesons in the momentum range $10 < p < 18$ GeV/c, $\Lambda^0/\bar{\Lambda}^0$ baryons in the momentum range $11.41 < p < 22.82$ GeV/c and neutral hadronic calorimeter clusters with $E > 15$ GeV, from which they have measured $A^s_{FB} = 0.131 \pm 0.035(stat.) \pm 0.013(syst.)$ and $A^{d,s}_{FB} = 0.112 \pm 0.031(stat.) \pm 0.054(syst.)$, respectively. However the extraction of the asymmetry parameters from the measured production asymmetries is model dependent. The OPAL collaboration has measured [4] the production asymmetries of a number of identified particle species with $x_p = 2p/E_{cm} \geq 0.5$, where E_{cm} denotes the center-of-mass energy in the event, and has determined most of the background contributions and analyzing powers from double-tagged events in the data. This eliminates most of the model dependence, but results in limited statistical precision, $A^u_{FB} = 0.040 \pm 0.067(stat.) \pm 0.028(syst.)$, $A^{d,s}_{FB} = 0.068 \pm 0.035(stat.) \pm 0.011(syst.)$.

In this paper we present a measurement of the asymmetry parameter for strange

quarks, A_s, using a sample of 300,000 hadronic Z^0 decays recorded by the SLD experiment at the SLAC Linear Collider between 1993 and 1997, with an average electron beam polarization of 74%. Hemispheres are tagged as s ($\bar{s}$) by the presence of a K^- (K^+) meson identified by the Cherenkov Ring Imaging Detector (CRID) or a Λ^0 ($\bar{\Lambda}^0$) hyperon tagged using a combination of flight distance and CRID information. The background from heavy flavor events ($c\bar{c}$ and $b\bar{b}$) was suppressed using lifetime information, allowing the use of relatively low-momentum identified kaons to tag s or $\bar{s}$ jets. The background from the other light flavors ($u\bar{u}$ and $d\bar{d}$) was suppressed by the additional requirement of a high-momentum identified strange particle in the opposite hemisphere of the event. This analysis is discussed in section 3. The asymmetry parameter was extracted from a simultaneous fit to the polar angle distributions measured with left- and right-handed electron beams, as discussed in section 4, which is insensitive to the initial state coupling. The analyzing power of the tags for true $s\bar{s}$ events, as well as the relative contribution of $u\bar{u} + d\bar{d}$ events were determined from the data as described in section 5. This procedure removes much of the model dependence, yielding an error that is statistically dominated.

2. Apparatus and Hadronic Event Selection

A general description of the SLD can be found elsewhere [5]. The trigger and initial selection criteria for hadronic Z^0 decays are described in Ref. [6]. This analysis used charged tracks measured in the Central Drift Chamber (CDC) [7] and Vertex Detector (VXD) [8], and identified using the Cherenkov Ring Imaging Detector (CRID) [9]. Momentum measurement is provided by a uniform axial magnetic field of 0.6T. The CDC and VXD give a momentum resolution of $\sigma_{p_\perp}/p_\perp = 0.01 \oplus 0.0026 p_\perp$, where $p_\perp$ is the track momentum transverse to the beam axis in GeV/c. One half of the data were taken with the original vertex detector (VXD2), and the other half with the upgraded detector (VXD3). In the plane normal to the beamline the centroid of

the micron-sized SLC interaction point (IP) was reconstructed from tracks in sets of approximately thirty sequential hadronic Z^0 decays to a precision of $\sigma_{IP} \simeq 7$ μm for the VXD2 data and $\simeq$5 μm for the VXD3 data. Including the uncertainty on the IP position, the resolution on the charged track impact parameter (d) projected in the plane perpendicular to the beamline is $\sigma_d = 11 \oplus 70/(p_\perp \sin^{3/2}\theta)$ μm for VXD2 and $\sigma_d = 9 \oplus 29/(p_\perp \sin^{3/2}\theta)$ μm for VXD3, where θ is the track polar angle with respect to the beamline. The CRID comprises two radiator systems that between them identify charged pions with high efficiency and purity in the momentum range 0.3–35 GeV/c, charged kaons in the ranges 0.75–6 GeV/c and 9–35 GeV/c, and protons in the ranges 0.75–6 GeV/c and 10–46 GeV/c [10]. The event thrust axis [11] was calculated using energy clusters measured in the Liquid Argon Calorimeter [12].

A set of cuts was applied to the data to select well-measured tracks and events well contained within the detector acceptance. Charged tracks were required to have a distance of closest approach transverse to the beam axis within 5 cm, and within 10 cm along the axis from the measured IP, as well as $|\cos\theta| < 0.80$, and $p_\perp > 0.15$ GeV/c. Events were required to have a minimum of seven such tracks, a thrust axis polar angle w.r.t. the beamline, θ_T, within $|\cos\theta_T| < 0.71$, and a charged visible energy E_{vis} of at least 20 GeV, which was calculated from the selected tracks assigned the charged pion mass. The efficiency for selecting a well-contained $Z^0 \to q\bar{q}(g)$ event was estimated to be above 96% independent of quark flavor.

In order to reduce the effects of decays of heavy hadrons, we selected light flavor events ($u\bar{u}$, $d\bar{d}$ and $s\bar{s}$) by requiring each high-quality [13] track in the event to have a transverse impact parameter with respect to the IP of less than three times its estimated error. Finally, the CRID was required to be operational. The selected sample comprised roughly 94,000 events, with an estimated background contribution of 13% from $c\bar{c}$ events, 1% from $b\bar{b}$ events, and a non-hadronic background contribution of 0.10 ± 0.05%, dominated by $Z^0 \to \tau^+\tau^-$ events.

For the purpose of estimating the efficiency and purity of the event flavor tagging

and the particle identification, we made use of a detailed Monte Carlo (MC) simulation of the detector. The JETSET 7.4 [14] event generator was used, with parameter values tuned to hadronic e^+e^- annihilation data [15], combined with a simulation of B-hadron decays tuned [16] to $\Upsilon(4S)$ data and a simulation of the SLD based on GEANT 3.21 [17]. Inclusive distributions of single-particle and event-topology observables in hadronic events were found to be well described by the simulation [6].

3. Selection of $s\bar{s}$ Events

After the event selection described in the previous section, $s\bar{s}$ events are selected by the presence of identified high-momentum $K^{\pm}$, K^0_s or $\Lambda^0/\bar{\Lambda}^0$. These particles are likely [2] to contain an initial $s/\bar{s}$ quark, but could also contain an initial u and/or d quark or be from the decay of a D or B hadron. In this analysis the strategy for reducing the model dependence of the result involves hard analysis cuts to suppress the non-$s\bar{s}$ background and enhance the analyzing power of the signal to a level where useful constraints can be obtained from the data.

The first step is the selection of strange particles. The CRID allows $K^{\pm}$ to be separated from $p/\bar{p}$ and $\pi^{\pm}$ with high purity for tracks with $p > 9$ GeV/c as described in detail in [10]. For the purpose of identifying $K^{\pm}$, relatively loose quality cuts are applied. Tracks with poor CRID information or that are likely to have scattered or interacted before exiting the CRID are removed by requiring each track to have at least 40 CDC hits, at least one of which is at a radius of at least 92 cm, to extrapolate through an active region of the CRID gas radiator and through a live CRID TPC. For the remaining tracks log-likelihoods [10, 18] are calculated for the CRID gas radiator for each of the three charged hadron hypotheses $\pi^{\pm}$, $K^{\pm}$ and $p/\bar{p}$. A track is tagged as a $K^{\pm}$ by the gas system if the log-likelihood for this hypothesis exceeds both of the other log-likelihoods by at least 3 units. Figure 1 shows the momentum distribution of identified $K^{\pm}$ for our data and Monte Carlo simulation. The shape of the data

distribution is well described by the simulation, however, the normalization of the simulated distribution for $p > 12$ GeV/c appears to be too low compared with the data. We correct this difference for a later comparison of quantities in the data and the simulation given below. We thus apply a momentum-independent normalization correction of 2.7% to the simulation in order to improve the overall agreement, and retain this correction for the studies in this and the following sections. The effect of this correction on the final result will be discussed in section 5. The average purity of the $K^{\pm}$ sample was estimated using the simulation to be 89%.

The selection of K^0_s and $\Lambda^0/\bar{\Lambda}^0$ is also described in detail in [10]. Briefly, K^0_s and $\Lambda^0/\bar{\Lambda}^0$ are reconstructed in the modes $K^0_s \to \pi^+\pi^-$ (BR $\approx$ 69%) and $\Lambda^0(\bar{\Lambda}^0) \to p(\bar{p})\pi^{\mp}$ (BR $\approx$ 64%) and are identified by their long flight distance, reconstructed mass, and accuracy of pointing back to the primary interaction point. K^0_s and $\Lambda^0/\bar{\Lambda}^0$ are required to have $p > 5$ GeV/c. Pairs of tracks with invariant mass $m_{\pi\pi}$ within 12 MeV/c^2 of the nominal K^0_s mass are identified as K^0_s. Figure 1 gives the momentum distribution for the K^0_s sample. The Monte Carlo simulation for the K^0_s momentum has an excess for low momenta. For the reason given in the previous paragraph, we correct this discrepancy in the simulation by applying a simple (linear) momentum-dependent correction factor to the number of simulated K^0_s candidates with $p < 15$ GeV/c; this procedure rejects a total of 4.6% of the simulated K^0_s sample. This correction is used in the following comparisons between data and simulation and its systematic effect will be discussed in section 5. The simulation predicts that the average purity of the K^0_s sample is 91%.

In the case of the $\Lambda^0/\bar{\Lambda}^0$, information from the Cherenkov Ring Imaging Detector is used to identify the $p/\bar{p}$ candidate. $\Lambda^0/\bar{\Lambda}^0$ are identified by requiring the invariant mass of pairs of tracks, $m_{p\pi}$, to be within 5 MeV/c^2 of the nominal $\Lambda^0/\bar{\Lambda}^0$ mass and at least one of the following sets of requirements to be passed: i.) the candidate is not contained within 36 MeV/c^2 of the nominal K^0_s mass, or ii.) the high-momentum track is identified as a proton by the particle ID system, or iii.) the candidate is

not contained within 12 MeV/c^2 of the nominal K^0_s mass and the pion hypothesis for the high-momentum track is rejected by the particle ID system. Figure 1 gives the momentum distribution for the $\Lambda^0/\bar{\Lambda}^0$ sample. The Monte Carlo simulation predicts too many low-momentum $\Lambda^0/\bar{\Lambda}^0$ candidates, and similar to the case in the K^0_s sample, we correct this discrepancy in the simulation by applying a simple (linear) momentum-dependent correction factor to the number of simulated $\Lambda^0/\bar{\Lambda}^0$ candidates with $p < 20$ GeV/c; this procedure rejects a total of 7.2% of the simulated $\Lambda^0/\bar{\Lambda}^0$ sample. Again, this correction is retained and its systematic effect will be discussed in section 5. The simulation predicts that the average purity of the $\Lambda^0/\bar{\Lambda}^0$ sample is 84%.

These strange particles are then used to tag s and $\bar{s}$ jets as follows. The event is divided into two hemispheres by a plane perpendicular to the thrust axis. We require each of the two hemispheres to contain at least one identified strange particle ($K^{\pm}$, K^0_s or $\Lambda^0/\bar{\Lambda}^0$); for hemispheres with multiple strange particles we only consider the one with the highest momentum. We require at least one of the two hemispheres to have definite strangeness (i.e. to contain a $K^{\pm}$ or $\Lambda^0/\bar{\Lambda}^0$). In events with two hemispheres of definite strangeness, the two hemispheres are required to have opposite strangeness (e.g. K^+K^-). This procedure increases the $s\bar{s}$ purity substantially compared with a single tag; thus, for these events, the model dependence of the measurement (section 4) is reduced. Table 1 summarizes the composition of the selected event sample for data and simulation for each of the 5 tagging modes used. The number of events for each mode shown is in good agreement with the Monte Carlo prediction. The $s\bar{s}$ purity and $s\bar{s}$ analyzing power were estimated from the simulation.

The $K^{\pm}K^{\mp}$ mode and the $K^{\pm}K^0_s$ mode dominate the sample and the $K^{\pm}K^{\mp}$ mode has the highest $s\bar{s}$ purity. The combined $s\bar{s}$ purity of all modes is 69%, and the predicted background in the selected event sample consists of 10% $u\bar{u}$, 9% $d\bar{d}$, 11% $c\bar{c}$, and 1% $b\bar{b}$ events.

Table 1: Summary of selected event sample for 5 modes in data and simulation.

Mode	Data	MC prediction	$s\bar{s}$ purity	$s\bar{s}$ analyzing power
K^+K^-	619	620	0.76	0.94
$K^+\Lambda^0, K^-\bar{\Lambda}^0$	86	82	0.65	0.86
$\Lambda^0\bar{\Lambda}^0$	1	6	0.59	
$K^\pm K_s^0$	502	531	0.64	0.68
$\Lambda^0 K_s^0, \bar{\Lambda}^0 K_s^0$	52	52	0.54	0.44
Total:	1260	1291	0.69	0.82

The analyzing power is defined as:

$$a_s = \frac{N_s^{right} - N_s^{wrong}}{N_s^{right} + N_s^{wrong}} \tag{4}$$

where $N_s^{right}(N_s^{wrong})$ denotes the number of $s\bar{s}$ events in which a particle of negative strangeness is found in the true $s(\bar{s})$ hemisphere. The average analyzing power for all modes is predicted by the simulation to be 0.82. The $K^\pm K^\mp$ mode has a substantially higher analyzing power than the other modes.

The initial s quark direction is approximated by the thrust axis, $\hat{t}$ of the event, signed to point in the direction of negative strangeness:

$$x = cos\theta_s = S\frac{\vec{p}\cdot\hat{t}}{|\vec{p}\cdot\hat{t}|}\hat{t}_z, \tag{5}$$

where S and $\vec{p}$ denote the strangeness and the momentum of the tagging particle.

Figure 2 shows the polar angle distributions, for all modes combined, of the signed thrust axis for left-handed ($P_e < 0$) and right-handed ($P_e > 0$) electron beams. The expected production asymmetries, of opposite sign for the left-handed and the right-handed beams, are clearly visible.

4. Extraction of A_s

A_s is extracted from these distributions by a binned maximum likelihood fit. The fitting function is given by:

$$P(x) = D(x) \sum_f N_f (1 + x^2 + 2(1+\delta) a_f A_f A_Z x). \tag{6}$$

Here, the function $D(x)$ describes the x-dependence of the acceptance and the strange particle identification efficiencies. $N_f = N_{events} R_f \epsilon_f$ denotes the number of events in the sample of flavor f ($f = u, d, s, c, b$) in terms of the number of selected hadronic events N_{events}, $R_f = \Gamma(Z^0 \to f\bar{f})/\Gamma(Z^0 \to hadrons)$ and the tagging efficiencies ϵ_f; $\delta = -0.013$ corrects for the effects of hard gluon radiation [19]; a_f denotes the analyzing power for tagging the f rather than the $\bar{f}$ direction; A_f is the asymmetry parameter for flavor f; and $A_Z = (A_e - P_e)/(1 - A_e P_e)$ (section 1).

The function $D(x)$ was calculated from the simulation and verified by comparing data and simulated x-distributions of identified $K^{\pm}$, K^0_s, and $\Lambda^0/\bar{\Lambda}^0$. The parameters ϵ_c, ϵ_b, and a_c, a_b for the heavy flavors are taken from the Monte Carlo simulation [16] since a number of independent measurements lead us to believe these parameters to be reliable within well defined uncertainties. The world average experimental measurements of the parameters A_c, A_b, R_c, R_b [1] were used. The corresponding systematic uncertainties are small and are discussed below.

For the light flavors, the relevant parameters in the fitting function are derived where possible from the data. The total number of light flavor events, N_{uds}, is determined by subtracting the number of heavy flavor events (obtained from the simulation) from the entire event sample. As discussed in the next section, the ratio N_{ud}/N_s is determined from the simulation to be 0.27 and constrained by data. The asymmetry parameters A_u and A_d are set to the Standard Model values. The $s\bar{s}$ analyzing power, a_s, is determined from the simulation to be 0.82 (averaged over all modes) and constrained by data (section 5). The combined $(u\bar{u} + d\bar{d})$ analyzing power, a_{ud}, is estimated to be -0.41 (section 5).

The result of the fit is shown as a histogram in Figure 2. The fit quality is good with a χ^2 of 12.9 for 24 bins. Also included are our estimates of non-$s\bar{s}$ background. The cross-hatched histograms indicate $c\bar{c} + b\bar{b}$ backgrounds which are seen to show asymmetries of the same sign and similar slope to the total distribution. The hatched histograms indicate $u\bar{u} + d\bar{d}$ backgrounds showing asymmetries of the opposite sign and slope to the total distribution. The A_s value extracted from the fit is $A_s = 0.82 \pm 0.10(stat.)$.

5. Systematic Errors and Checks

The understanding of the parameters used as inputs to the fitting function and of their uncertainties is crucial to this analysis. The characteristics of heavy flavor events relevant to this analysis have been measured experimentally, and our simulation [14, 15, 17] has been tuned [16] to reproduce these results. The effect of uncertainties in the values of R_c, R_b, A_c and A_b were evaluated by varying those parameters by the uncertainties on their world average values [1]. Uncertainties in other measured quantities such as the D and B hadron fragmentation functions, the number of K^- and K^+ mesons produced per D or B hadron decay, as well as a number of other quantities [6] were taken into account by varying each quantity in turn by plus and minus the error on its world average value. The sum in quadrature of these uncertainties was taken as the systematic error due to heavy flavor modelling and is listed in Table 2. This is a relatively small contribution to the total systematic error. Other small contributions to the systematic error include those from the 0.6% uncertainty in the correction for the effect of hard gluon radiation, and the 0.8% uncertainty in the beam polarization.

For the light flavors, there are few experimental constraints on the relevant input parameters. Qualitative features such as leading particle production [2], short range rapidity correlations between high-momentum KK and baryon-antibaryon pairs [20] and long-range correlations between several particle species [20] have been observed

experimentally, but these results are not sufficient to quantify the analyzing power of the strange-particle tag or the $u\bar{u}$ and $d\bar{d}$ background. Our Monte Carlo simulation provides a reasonable description of the above observations, and we have used our data to constrain the relevant input parameters in the context of our Monte Carlo model.

For the analyzing power in $s\bar{s}$ events, we note that there are only two ways to mis-tag an s jet as an $\bar{s}$ jet: either the jet must contain a true K^+ or $\bar{\Lambda}^0$ that satisfies our cuts, or we must mis-identify a π^+ or p as a K^+ or reconstruct a fake $\bar{\Lambda}^0$. The Monte Carlo simulation predicts that the fraction of events with a mis-identified particle is negligible in tagged $s\bar{s}$ events, since the majority of high-momentum tracks in these events are kaons, and the relative V^0 fake rate is low. We have measured our mis-identification rates in the data [10], and they contribute less than 0.2% to the wrong sign fraction, so we neglect this source of systematic uncertainty.

If a high-momentum K^+ is produced in an s jet, then there must be an associated strange particle in the jet, which will also tend to have high momentum. Including the leading strange particle, such a jet will contain one antistrange and two strange particles, all with relatively high momentum. We can therefore investigate the rate of production of these wrong-sign kaons by studying events in which we find three identified $K^{\pm}$ and/or K^0_s. Such events are expected to be fairly pure in $s/\bar{s}$, since a $u/\bar{u}$ or $d/\bar{d}$ jet would have to contain either four strange particles or two strange particles and one mis-identified particle in order to be selected. In order to obtain higher statistics for this study, we loosened the momentum cut on charged kaons to $p > 8$ GeV/c and did not require separation from protons for tracks with $8 < p < 11$ GeV/c. In our data we found 94 hemispheres containing three identified $K^{\pm}$ and/or K^0_s, compared with a Monte Carlo prediction of 99. We subtracted the simulated non-s jet background of 37 events to yield a measured number of 57 ± 10 jets with 3 kaons, providing an 18% constraint on the number of $s\bar{s}$ events that *could* have the wrong sign. Since the Monte Carlo prediction is consistent with the data, we used the simulated $a_s = 0.82$ as our central value for the analyzing power in $s\bar{s}$ events.

This constraint is not entirely model-independent, since we are relying on the model to predict the fraction of these jets in which all three kaons pass our momentum cuts, as well as the fraction in which the wrong-sign kaon is chosen as the tagging particle rather than either of the right-sign kaons. Therefore, we conservatively applied the 18% uncertainty to the wrong-sign fraction, resulting in a 4% uncertainty on A_s, as shown in Table 2. We repeated this check with our standard charged kaon selection, and also counted hemispheres containing a K^+K^+ or K^-K^- pair, obtaining consistent but less precise constraints.

Table 2: Summary of systematic uncertainties.

Source	Comments	Systematic variation	$\delta A_s/A_s$
heavy flavor modelling	MC/world averages	Ref. [1, 15, 16]	0.008
hard gluon radiation	Stav-Olsen with bias correction	$(1.3 \pm 0.6)\%$	0.006
beam polarization	data	$(73.7 \pm 0.8)\%$	0.008
a_s	MC constrained by 3 K jets in data	0.82 ± 0.03	0.038
a_{ud}	$-a_s < a_{ud} < 0$	-0.41 ± 0.24	0.071
A_{ud}	Standard Model	–	–
N_{ud}/N_s	MC constrained by 2 K jets in data	0.27 ± 0.03	0.037
p distribution correction		(see text)	–
Total:			0.089

The relative $u\bar{u} + d\bar{d}$ background level N_{ud}/N_s was constrained from the data by exploiting the fact that an even number of strange particles must be produced in a u/d jet, and that they appear in strange-antistrange pairs that have similar momenta.

We counted 585 hemispheres in the data containing an identified K^+-K^- pair and 387 hemispheres containing an identified $K^\pm$-K^0 pair. The respective Monte Carlo predictions of 578 and 377 are consistent. After subtracting the predicted non-u/d jet backgrounds, both of these two checks yielded 12% constraints on the $u\bar{u} + d\bar{d}$ background. We also counted events in the data that were tagged by kaons of the same sign in both hemispheres. The Monte Carlo prediction is consistent, but the constraint obtained is less precise. Again, we have used the Monte Carlo central value and, since the constraints are not completely model-independent, we have used the most precise one to estimate the systematic error.

The above checks are also sensitive to the analyzing power of $u\bar{u} + d\bar{d}$ events, a_{ud}. However, with the present event statistics we cannot obtain a tight constraint on this quantity. We therefore assume that a_{ud} must be negative, since u and d jets must produce a leading K^+ rather than K^-, and that the modulus of a_{ud} must be less than that of a_s, since there is always a companion particle of opposite strangeness in a u or d jet that will tend to dilute the analyzing power. We take these as hard limits, $-0.82 < a_{ud} < 0$, use the middle of the range for our central value and assign an uncertainty equal to the range divided by $\sqrt{12}$. The simulation predicts a value of $a_{ud} = -0.38$, consistent with our estimate.

The effects on the central value of A_s due to the corrections (section 3) of the Monte Carlo $K^\pm$, K^0_s and $\Lambda^0/\bar{\Lambda}^0$ momentum distributions were studied. It was determined that the changes in the $s\bar{s}$ purity and the analyzing power in $s\bar{s}$ events were small. The change in the central value of A_s when these corrections were removed was smaller than any of the contributions listed in Table 2 and we considered it negligible. The individual systematic errors were added in quadrature to yield a total systematic error of $\delta A_s/A_s = 0.089$, i.e. $\delta A_s = 0.07$.

6. Summary and Conclusion

We have presented a preliminary direct measurement of the parity violating coupling of the Z^0 to strange quarks, A_s, derived from a sample of approximately 300,000 hadronic decays of Z^0 bosons produced with a polarized electron beam and recorded by the SLD experiment at SLAC between 1993 and 1997. The precision CCD vertex detector allows the suppression of the heavy flavor background, and the Cherenkov Ring Imaging Detector is crucial in the tagging of high-momentum $K^{\pm}$ and helps improve the $\Lambda^0/\bar{\Lambda}^0$ purity. The coupling A_s is obtained directly from a measurement of the left-right-forward-backward production asymmetry in polar angle of the tagged s quark. The background from $u\bar{u}$ and $d\bar{d}$ events is measured from the data, as is the analyzing power of the method for $s\bar{s}$ events.

A binned maximum likelihood fit is used to obtain the result:

$$A_s = 0.82 \pm 0.10(stat.) \pm 0.07(syst.)(preliminary). \tag{7}$$

This result is consistent with the Standard Model expectation for A_s. Our measurement can be used to test the universality of the coupling constants by comparing it with the world average value for A_b [1]. The two measurements are consistent.

In order to compare with previous measurements of A^s_{FB} and $A^{d,s}_{FB}$ (see section 1), we must assume a value of A_e. Using $A_e = 0.1499$ [1] and neglecting the small uncertainty on A_e, the DELPHI measurements translate into $A_s = 1.165 \pm 0.311(stat.) \pm 0.116(syst.)$ and $A_{d,s} = 0.996 \pm 0.276(stat.) \pm 0.480(syst.)$. Similarly, the OPAL measurement yields $A_{d,s} = 0.605 \pm 0.311(stat.) \pm 0.098(syst.)$. Our measurement is consistent with these and represents a substantial improvement in precision.

Acknowledgements

We thank the personnel of the SLAC accelerator department and the technical staffs of our collaborating institutions for their outstanding efforts on our behalf.

*Work supported by Department of Energy contracts: DE-FG02-91ER40676 (BU), DE-FG03-91ER40618 (UCSB), DE-FG03-92ER40689 (UCSC), DE-FG03-93ER40788 (CSU), DE-FG02-91ER40672 (Colorado), DE-FG02-91ER40677 (Illinois), DE-AC03-76SF00098 (LBL), DE-FG02-92ER40715 (Massachusetts), DE-FC02-94ER40818 (MIT), DE-FG03-96ER40969 (Oregon), DE-AC03-76SF00515 (SLAC), DE-FG05-91ER40627 (Tennessee), DE-FG02-95ER40896 (Wisconsin), DE-FG02-92ER40704 (Yale); National Science Foundation grants: PHY-91-13428 (UCSC), PHY-89-21320 (Columbia), PHY-92-04239 (Cincinnati), PHY-95-10439 (Rutgers), PHY-88-19316 (Vanderbilt), PHY-92-03212 (Washington); The UK Particle Physics and Astronomy Research Council (Brunel, Oxford and RAL); The Istituto Nazionale di Fisica Nucleare of Italy (Bologna, Ferrara, Frascati, Pisa, Padova, Perugia); The Japan-US Cooperative Research Project on High Energy Physics (Nagoya, Tohoku); The Korea Research Foundation (Soongsil, 1997).

References

[1] LEPEWWG/98-01, ALEPH 98-037 PHYSICS 98-018, DELPHI 98-46 PHYS 774, L3 Note 2259, OPAL Technical Note TN 541, SLD Physics Note 68 (1998).

[2] SLD Collaboration, K. Abe et al., Phys. Rev. Lett. **78** (1997) 3442.

[3] DELPHI Collaboration, P. Abreu et al., Z. Phys. **C67** (1995) 1.

[4] OPAL Collaboration, K. Ackerstaff et al., Z. Phys. **C76** (1997) 387.

[5] SLD Design Report, SLAC-Report 273 (1984).

[6] SLD Collaboration: K. Abe et al., Phys. Rev. **D51** (1995) 962.

[7] M. D. Hildreth et al., Nucl. Instr. Meth. **A367** (1995) 111.

[8] C.J.S. Damerell et. al., Nucl. Instr. Meth. **A288** (1990) 236.
C.J.S. Damerell et. al., Nucl. Instr. Meth. **A400** (1997) 287.

[9] K. Abe et al., Nucl. Inst. Meth. **A343** (1994) 74.

[10] K. Abe et al., SLAC-PUB-7766, submitted to Phys. Rev. D and contributed to this conference.

[11] S. Brandt et al., Phys. Lett. **12** (1964) 57.
E. Farhi, Phys. Rev. Lett. **39** (1977) 1587.

[12] D. Axen et al., Nucl. Inst. Meth. **A328** (1993) 472.

[13] SLD Collaboration, K. Abe et al., Phys. Rev. **D53** (1996) 1023.

[14] T. Sjöstrand, Comput. Phys. Commun. **82** (1994) 74.

[15] P. N. Burrows, Z. Phys. **C41** (1988) 375.
OPAL Collaboration, M.Z. Akrawy et al., Z. Phys. **C47** (1990) 505.

[16] SLD Collaboration, K. Abe et al., Phys. Rev. Lett. **79** (1997) 590.

[17] R. Brun et al., Report No. CERN-DD/EE/84-1 (1989).

[18] K. Abe et al., Nucl. Inst. and Meth. **A371** (1996) 195.

[19] J. B. Stav and H. A. Olsen, Phys. Rev. **D52** (1995) 1359.

[20] K. Abe et al., SLAC-PUB-7824, contributed to this conference.

**List of Authors

K. Abe,[2] K. Abe,[19] T. Abe,[27] I.Adam,[27] T. Akagi,[27] N. J. Allen,[4]
A. Arodzero,[20] W.W. Ash,[27] D. Aston,[27] K.G. Baird,[15] C. Baltay,[37]
H.R. Band,[36] M.B. Barakat,[14] O. Bardon,[17] T.L. Barklow,[27] J.M. Bauer,[16]
G. Bellodi,[21] R. Ben-David,[37] A.C. Benvenuti,[3] G.M. Bilei,[23] D. Bisello,[22]
G. Blaylock,[15] J.R. Bogart,[27] B. Bolen,[16] G.R. Bower,[27] J. E. Brau,[20]
M. Breidenbach,[27] W.M. Bugg,[30] D. Burke,[27] T.H. Burnett,[35] P.N. Burrows,[21]
A. Calcaterra,[11] D.O. Caldwell,[32] D. Calloway,[27] B. Camanzi,[10]
M. Carpinelli,[24] R. Cassell,[27] R. Castaldi,[24] A. Castro,[22] M. Cavalli-Sforza,[33]
A. Chou,[27] E. Church,[35] H.O. Cohn,[30] J.A. Coller,[5] M.R. Convery,[27]
V. Cook,[35] R. Cotton,[4] R.F. Cowan,[17] D.G. Coyne,[33] G. Crawford,[27]
C.J.S. Damerell,[25] M. N. Danielson,[7] M. Daoudi,[27] N. de Groot,[27]

R. Dell'Orso,[23] P.J. Dervan,[4] R. de Sangro,[11] M. Dima,[9] A. D'Oliveira,[6]
D.N. Dong,[17] P.Y.C. Du,[30] R. Dubois,[27] B.I. Eisenstein,[12] V. Eschenburg,[16]
E. Etzion,[36] S. Fahey,[7] D. Falciai,[11] C. Fan,[7] J.P. Fernandez,[33] M.J. Fero,[17]
K.Flood,[15] R. Frey,[20] T. Gillman,[25] G. Gladding,[12] S. Gonzalez,[17]
E.L. Hart,[30] J.L. Harton,[9] A. Hasan,[4] K. Hasuko,[31] S. J. Hedges,[5]
S.S. Hertzbach,[15] M.D. Hildreth,[27] J. Huber,[20] M.E. Huffer,[27] E.W. Hughes,[27]
X.Huynh,[27] H. Hwang,[20] M. Iwasaki,[20] D. J. Jackson,[25] P. Jacques,[26]
J.A. Jaros,[27] Z.Y. Jiang,[27] A.S. Johnson,[27] J.R. Johnson,[36] R.A. Johnson,[6]
T. Junk,[27] R. Kajikawa,[19] M. Kalelkar,[26] Y. Kamyshkov,[30] H.J. Kang,[26]
I. Karliner,[12] H. Kawahara,[27] Y. D. Kim,[28] R. King,[27] M.E. King,[27]
R.R. Kofler,[15] N.M. Krishna,[7] R.S. Kroeger,[16] M. Langston,[20] A. Lath,[17]
D.W.G. Leith,[27] V. Lia,[17] C.-J. S. Lin,[27] X. Liu,[33] M.X. Liu,[37] M. Loreti,[22]
A. Lu,[32] H.L. Lynch,[27] J. Ma,[35] G. Mancinelli,[26] S. Manly,[37] G. Mantovani,[23]
T.W. Markiewicz,[27] T. Maruyama,[27] H. Masuda,[27] E. Mazzucato,[10]
A.K. McKemey,[4] B.T. Meadows,[6] G. Menegatti,[10] R. Messner,[27]
P.M. Mockett,[35] K.C. Moffeit,[27] T.B. Moore,[37] M.Morii,[27] D. Muller,[27]
V.Murzin,[18] T. Nagamine,[31] S. Narita,[31] U. Nauenberg,[7] H. Neal,[27]
M. Nussbaum,[6] N.Oishi,[19] D. Onoprienko,[30] L.S. Osborne,[17] R.S. Panvini,[34]
H. Park,[20] C. H. Park,[29] T.J. Pavel,[27] I. Peruzzi,[11] M. Piccolo,[11]
L. Piemontese,[10] E. Pieroni,[24] K.T. Pitts,[20] R.J. Plano,[26] R. Prepost,[36]
C.Y. Prescott,[27] G.D. Punkar,[27] J. Quigley,[17] B.N. Ratcliff,[27] T.W. Reeves,[34]
J. Reidy,[16] P.L. Reinertsen,[33] P.E. Rensing,[27] L.S. Rochester,[27] P.C. Rowson,[8]
J.J. Russell,[27] O.H. Saxton,[27] T. Schalk,[33] R.H. Schindler,[27] B.A. Schumm,[33]
J. Schwiening,[27] S. Sen,[37] V.V. Serbo,[36] M.H. Shaevitz,[8] J.T. Shank,[5]
G. Shapiro,[13] D.J. Sherden,[27] K. D. Shmakov,[30] C. Simopoulos,[27] N.B. Sinev,[20]
S.R. Smith,[27] M. B. Smy,[9] J.A. Snyder,[37] H. Staengle,[9] A. Stahl,[27]
P. Stamer,[26] R. Steiner,[1] H. Steiner,[13] M.G. Strauss,[15] D. Su,[27] F. Suekane,[31]
A. Sugiyama,[19] S. Suzuki,[19] M. Swartz,[27] A. Szumilo,[35] T. Takahashi,[27]
F.E. Taylor,[17] J. Thom,[27] E. Torrence,[17] N. K. Toumbas,[27] A.I. Trandafir,[15]
J.D. Turk,[37] T. Usher,[27] C. Vannini,[24] J. Va'vra,[27] E. Vella,[27] J.P. Venuti,[34]
R. Verdier,[17] P.G. Verdini,[24] S.R. Wagner,[27] D. L. Wagner,[7] A.P. Waite,[27]
Walston, S.,[20] J.Wang,[27] C. Ward,[4] S.J. Watts,[4] A.W. Weidemann,[30]
E. R. Weiss,[35] J.S. Whitaker,[5] S.L. White,[30] F.J. Wickens,[25] B. Williams,[7]
D.C. Williams,[17] S.H. Williams,[27] S. Willocq,[27] R.J. Wilson,[9]
W.J. Wisniewski,[27] J. L. Wittlin,[15] M. Woods,[27] G.B. Word,[34] T.R. Wright,[36]
J. Wyss,[22] R.K. Yamamoto,[17] J.M. Yamartino,[17] X. Yang,[20] J. Yashima,[31]
S.J. Yellin,[32] C.C. Young,[27] H. Yuta,[2] G. Zapalac,[36] R.W. Zdarko,[27]

J. Zhou.[20]

(The SLD Collaboration)

[1] *Adelphi University, South Avenue- Garden City,NY 11530,*
[2] *Aomori University, 2-3-1 Kohata, Aomori City, 030 Japan,*
[3] *INFN Sezione di Bologna, Via Irnerio 46 I-40126 Bologna (Italy),*
[4] *Brunel University, Uxbridge, Middlesex - UB8 3PH United Kingdom,*
[5] *Boston University, 590 Commonwealth Ave. - Boston,MA 02215,*
[6] *University of Cincinnati, Cincinnati,OH 45221,*
[7] *University of Colorado, Campus Box 390 - Boulder,CO 80309,*
[8] *Columbia University, Nevis Laboratories P.O.Box 137 - Irvington,NY 10533,*
[9] *Colorado State University, Ft. Collins,CO 80523,*
[10] *INFN Sezione di Ferrara, Via Paradiso,12 - I-44100 Ferrara (Italy),*
[11] *Lab. Nazionali di Frascati, Casella Postale 13 I-00044 Frascati (Italy),*
[12] *University of Illinois, 1110 West Green St. Urbana,IL 61801,*
[13] *Lawrence Berkeley Laboratory, Dept.of Physics 50B-5211 University of California-Berkeley,CA 94720,*
[14] *Louisiana Technical University, ,*
[15] *University of Massachusetts, Amherst,MA 01003,*
[16] *University of Mississippi, University,MS 38677,*
[17] *Massachusetts Institute of Technology, 77 Massachussetts Avenue Cambridge,MA 02139,*
[18] *Moscow State University, Institute of Nuclear Physics 119899 Moscow Russia,*
[19] *Nagoya University, Nagoya 464 Japan,*
[20] *University of Oregon, Department of Physics Eugene,OR 97403,*
[21] *Oxford University, Oxford, OX1 3RH, United Kingdom,*
[22] *Universita di Padova, Via F. Marzolo,8 I-35100 Padova (Italy),*
[23] *Universita di Perugia, Sezione INFN, Via A. Pascoli I-06100 Perugia (Italy),*
[24] *INFN, Sezione di Pisa, Via Livornese,582/AS Piero a Grado I-56010 Pisa (Italy),*
[25] *Rutherford Appleton Laboratory, Chiton,Didcot - Oxon OX11 0QX United Kingdom,*
[26] *Rutgers University, Serin Physics Labs Piscataway,NJ 08855-0849,*
[27] *Stanford Linear Accelerator Center, 2575 Sand Hill Road Menlo Park,CA 94025,*
[28] *Sogang University, Ricci Hall Seoul, Korea,*
[29] *Soongsil University, Dongjakgu Sangdo 5 dong 1-1 Seoul, Korea 156-743,*
[30] *University of Tennessee, 401 A.H. Nielsen Physics Blg. - Knoxville,Tennessee 37996-1200,*
[31] *Tohoku University, Bubble Chamber Lab. - Aramaki - Sendai 980 (Japan),*
[32] *U.C. Santa Barbara, 3019 Broida Hall Santa Barbara,CA 93106,*
[33] *U.C. Santa Cruz, Santa Cruz,CA 95064,*
[34] *Vanderbilt University, Stevenson Center,Room 5333 P.O.Box 1807,Station B Nashville,TN 37235,*

[35] *University of Washington, Seattle, WA 98105,*
[36] *University of Wisconsin, 1150 University Avenue Madison, WS 53706,*
[37] *Yale University, 5th Floor Gibbs Lab. - P.O.Box 208121 - New Haven, CT 06520-8121.*

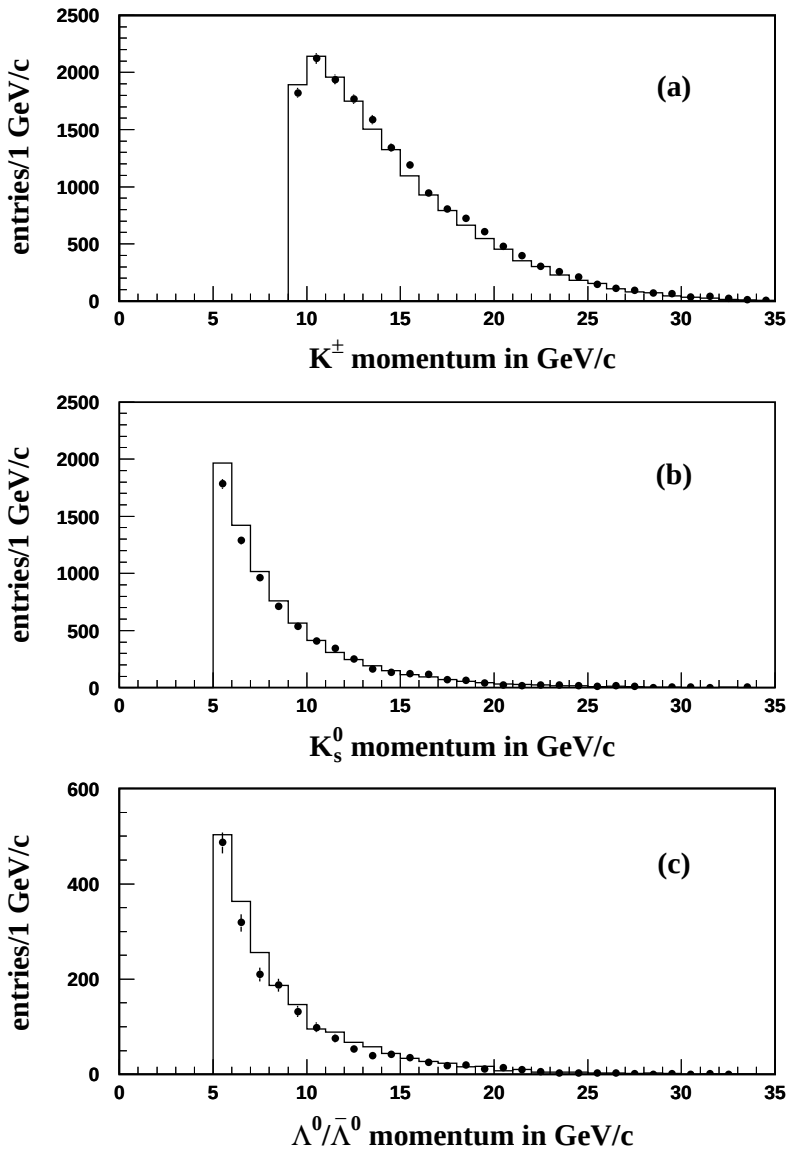

Figure 1: Momentum distributions for selected (a) $K^{\pm}$, (b) K^0_s and (c) $\Lambda^0/\bar{\Lambda}^0$ candidates in the data (dots). Also shown is the Monte Carlo simulation (histogram). The Monte Carlo distributions were later corrected, as described in the text.

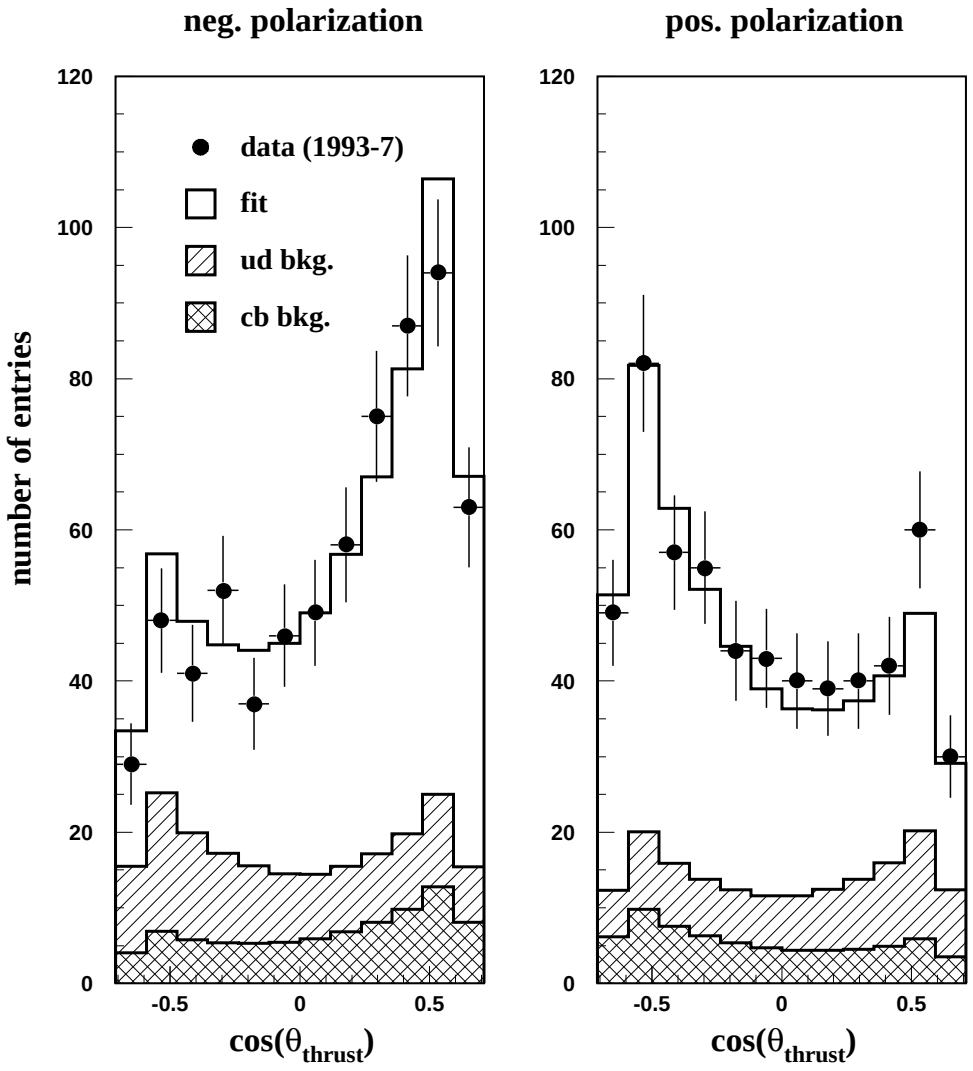

Figure 2: Polar angle distributions of the thrust axis, signed to point in the direction of negative strangeness, of the tagged strange particle, for negative (left) and positive (right) beam polarization. The dots show data and the histogram shows our fit to the data. Our estimates of the non-$s\bar{s}$ backgrounds are indicated by the shaded histograms.